

Spin-lattice relaxation time of conduction electrons in MgB₂

F. Simon,* F. Murányi,† T. Fehér, and A. Jánossy

*Institute of Physics and Condensed Matter Research Group of the Hungarian Academy of Sciences,
Budapest University of Technology and Economics, H-1521 Budapest, P.O. Box 91, Hungary*

L. Forró

IPMC/SB Swiss Federal Institute of Technology (EPFL), CH-1015 Lausanne-EPFL, Switzerland

C. Petrovic,‡ S. L. Bud'ko, and P. C. Canfield

*Ames Laboratory, U.S. Department of Energy and Department of Physics and Astronomy, Iowa State University, Ames,
Iowa 50011, USA*

(Received 3 April 2007; revised manuscript received 8 May 2007; published 26 July 2007)

The spin-lattice relaxation time, T_1 , of conduction electrons is measured as a function of temperature and magnetic field in MgB₂ in the normal and superconducting states. The method is based on the detection of the z component of the conduction electron magnetization under electron-spin-resonance conditions with amplitude-modulated microwave excitation. Measurement of T_1 below T_c at 0.32 T allows us to disentangle contributions from the two Fermi surfaces of MgB₂, as this field restores the normal state on the part of the Fermi surface with π symmetry only.

DOI: [10.1103/PhysRevB.76.024519](https://doi.org/10.1103/PhysRevB.76.024519)

PACS number(s): 74.70.Ad, 74.25.Nf, 76.30.Pk, 74.25.Ha

I. INTRODUCTION

The conduction electron spin-lattice relaxation time in metals, T_1 , is the characteristic time for the return to thermal equilibrium of a spin system driven out of equilibrium by, e.g., a microwave field at electron-spin resonance (ESR) or a spin-polarized current. The applicability of metals in “spintronics” devices in which information is processed using electron spins¹ depends on a sufficiently long spin lifetime. In pure metals T_1 is limited by the Elliott mechanism,^{2,3} i.e., the scattering of conduction electrons by the random spin-orbit potential of nonmagnetic impurities or phonons. In superconductors, the Elliott mechanism becomes ineffective and a long T_1 is predicted well below T_c .³ Here we report the direct measurement of the spin-lattice relaxation time of conduction electrons in MgB₂ in the superconducting state. The motivation to study the magnetic field and temperature dependence of T_1 is twofold: (i) to test the predicted lengthening of T_1 to temperatures well below T_c , and (ii) to measure the contributions to T_1 from different Fermi surface sheets and to compare with the corresponding momentum lifetimes.

The lengthening of T_1 has been observed in a restricted temperature range below T_c in the fulleride superconductor K₃C₆₀ by measuring the conduction electron-spin resonance (CESR) linewidth ΔH .⁴ This method assumes $1/T_1 = 1/T_2 = \gamma_e \Delta H$, where $\gamma_e/2\pi = 28.0$ GHz/T is the electron gyromagnetic ratio, and $1/T_2$ is the spin-spin or transversal relaxation rate. It is limited to cases where the homogeneous broadening of the CESR line due to a finite spin lifetime outweighs ΔH_{inhom} , the line broadening from inhomogeneities of the magnetic field. In a superconducting powder sample, the CESR line is inhomogeneously broadened below the irreversibility line due to the distribution of vortices, which is temperature and magnetic field dependent. This prevents the measurement of T_1 from the linewidth and calls for a method

to directly measure T_1 . Electron-spin echo techniques, which usually enable the measurement of T_1 , are not available for the required nanosecond time resolution range. The magnetic resonance technique, termed longitudinally detected (LOD) ESR,^{5,6} used in this work allows us to measure T_1 's as short as a few nanoseconds. The method is based on the measurement of the electron-spin magnetization along the magnetic field M_z , using modulated microwave excitation. M_z recovers to its equilibrium value with the T_1 time constant; thus the method allows the direct measurement of T_1 independent of magnetic field inhomogeneities.

MgB₂ has a high superconducting transition temperature⁷ of $T_c = 39$ K and its unusual physical properties^{8–11} are attributed^{12,13} to its disconnected, weakly interacting Fermi surface (FS) parts. The Fermi surface sheets derived from B orbitals with π and σ character (π and σ FSs) have smaller and higher electron-phonon couplings and superconductor gaps, respectively, and contribute roughly equally to the density of states (DOS). The strange band structure leads to unique thermodynamic properties: magnetic fields of about 0.3–0.4 T restore the π FS for all field orientations in polycrystalline samples but the material remains superconducting to much higher fields.^{9,10} This is characterized by a small and nearly isotropic upper critical field $H_{c2}^{\pi} \sim 0.3$ –0.4 T,^{10,14} and a strongly anisotropic one $H_{c2}^{\sigma} = 2$ –16 T,^{10,15,16} related to the π and σ Fermi surface sheets, respectively. Our measurements at low fields and low temperatures determine T_1 from the π FS alone, while high-field and high-temperature experiments measure T_1 averaged over the whole FS. We find that spin relaxation in high-purity MgB₂ is temperature independent in the high-field normal state between 3 and 50 K, indicating that it arises from nonmagnetic impurities. Spin relaxation times for electrons on the π and σ Fermi surface sheets are widely different but are not proportional to the corresponding momentum relaxation times.

II. EXPERIMENT

The same MgB_2 samples were used as in a previous study.¹⁷ Thorough grinding, particle size selection, and mixing with SnO_2 , an ESR-silent oxide, produced a fine powder with well-separated small metallic particles. The nearly symmetric appearance of the CESR signal¹⁸ proves that penetration of microwaves is homogeneous and that the particles are smaller than the microwave penetration depth of $\sim 1 \mu\text{m}$. Superconducting quantum interference device magnetometry showed that grinding and particle selection do not affect the superconducting properties. The particles are not single crystals but rather aggregates of small-sized single crystals. Continuous wave (cw) and longitudinally detected ESR experiments were performed in a home-built apparatus⁶ at 9.1 and 35.4 GHz microwave frequencies, corresponding to 0.32 and 1.27 T resonance magnetic fields. The 9.1 GHz apparatus is based on a loop-gap resonator with a low quality factor ($Q \sim 200$) and the 35.4 GHz instrument does not employ a microwave cavity at all. The cw ESR was detected using an audio frequency magnetic field modulation. Linewidths are determined by Lorentzian fits to the cw ESR data. For the LOD ESR, the microwaves are amplitude modulated with $f = \Omega/2\pi$ of typically 10 MHz, and the resulting varying M_z component of the sample magnetization is detected with a coil which is parallel to the external magnetic field and is part of a resonant circuit that is tuned to f and is matched to 50Ω . cw ESR at 420 GHz (centered at 15.0 T) was performed at EPFL using a quasi-optical microwave bridge with no resonant cavities.

III. RESULTS

A. Relaxation in the normal state

The low-temperature behavior of the spin-lattice relaxation time in MgB_2 in the normal state can be measured using cw ESR from the homogeneous linewidth ΔH_{hom} , using $1/T_1 = \gamma_e \Delta H_{\text{hom}}$ at high fields $H > H_{c2}$ that suppress superconductivity. The maximum upper critical field is $H_{c2,\text{max}} \sim 16$ T for particles with field in the (a, b) crystallographic plane in the polycrystalline sample at zero temperature.¹⁹ We did not observe any effects of superconductivity on the CESR; at 15 T it is suppressed in the full sample above a temperature of a few kelvin. Figure 1 shows that the temperature dependence of the CESR linewidth at 15 T is small below 40 K.

The CESR linewidth is magnetic field dependent as shown in Fig. 2 at 40 K: it is linear as a function of magnetic field with $\Delta H = \Delta H_0 + bH$, where $\Delta H_0 = 0.90(1)$ mT is the residual linewidth and $b = 0.057(1)$ mT/T. The field dependence probably originates from a g -factor anisotropy of the polycrystalline sample. The residual homogeneous linewidth corresponds to $T_1 = 6.3$ ns at 40 K. The linear relation can be used to correct the 15 T CESR linewidth data to obtain the homogeneous contribution $\Delta H_{\text{hom}}(T) = \Delta H(15 \text{ T}, T) - 15 \text{ T} \times b$ as the magnetic field dependence is expected to be temperature independent. We show the homogeneous linewidth in Fig. 1. We find that it is temperature independent within experimental precision between 3 and 50 K. This means that

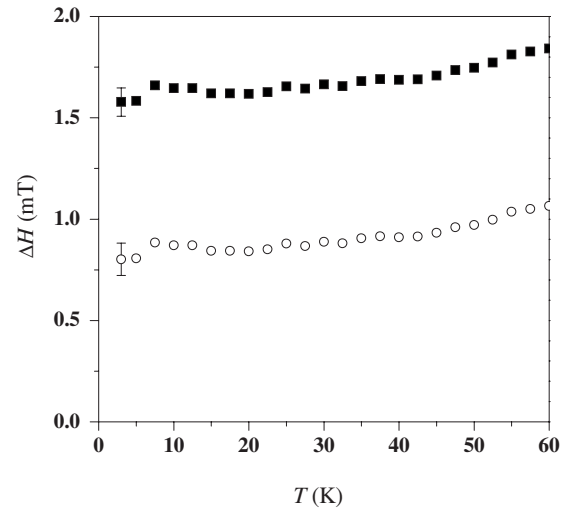


FIG. 1. CESR linewidth of MgB_2 as a function of temperature for the 15 T CESR measurement (■). Open circles (○) show the homogeneous linewidth (ΔH_{hom}) after correcting for the field-dependent broadening as explained in the text. Representative error bars are shown at the lowest temperature.

the spin-lattice relaxation time flattens to a residual value that is given by nonmagnetic impurities.

B. Relaxation in the superconducting state

In type II superconductors, CESR arises from thermal excitations and from normal state vortex cores. The inhomogeneity of the magnetic field in the vortex lattice or glass state does not broaden the CESR line. The local magnetic field inhomogeneity is averaged since within the spin lifetime itinerant electrons travel long distances compared to the intervortex distance.⁴ This is in contrast to the NMR case where the line shape is affected: the nuclei are fixed to the crystal and nuclei inside and outside the vortex cores experience different local fields.²⁰ In other words, a superconducting

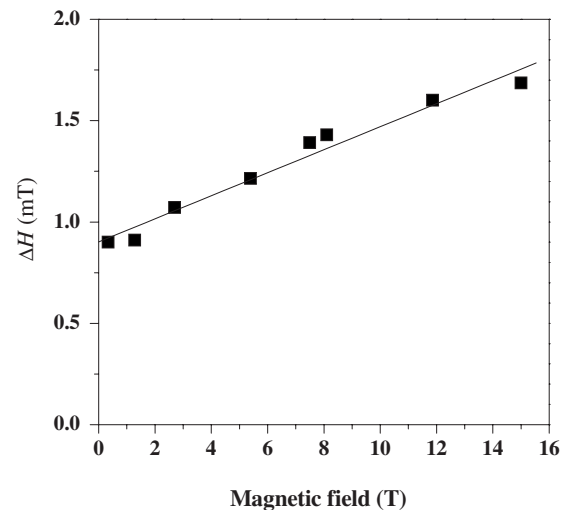


FIG. 2. ESR linewidth of MgB_2 as a function of magnetic field measured at 40 K (■). Solid curve is a linear fit to the data with parameters given in the text.

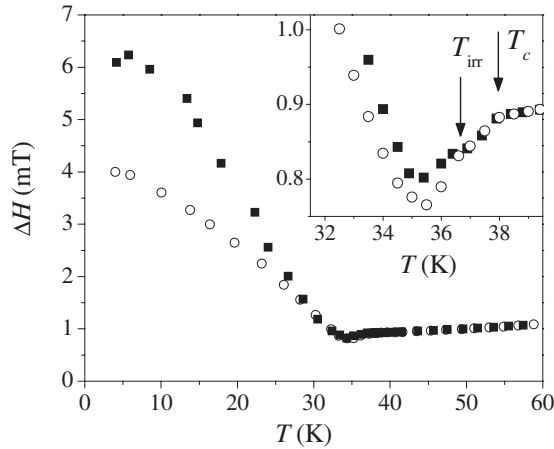


FIG. 3. Inhomogeneous CESR line broadening in MgB_2 below T_c at 0.32 T. Full and open symbols show the CESR linewidth for up and down magnetic field sweeps, respectively. Inset shows the data near T_c . Note the line narrowing below T_c and the field sweep direction dependent linewidths below the irreversibility temperature T_{irr} .

single-crystal sample would display a narrow conduction electron ESR line if there were no irreversible effects. However, the CESR line is inhomogeneously broadened below the irreversibility line for a superconducting powder sample: the vortex distribution depends on a number of factors such as the thermal and magnetic field history, grain size, and, for an anisotropic superconductor such as MgB_2 , the crystal orientation with respect to the magnetic field also. The resulting inhomogeneous broadening of the CESR line gives $1/\gamma\Delta H_{\text{inhom}} = T_2^* \ll T_{1,2}$, and T_1 cannot be measured from the linewidth. In Fig. 3 we show this effect: above T_c MgB_2 has a relaxationally broadened linewidth of $\Delta H = 0.9$ mT. Between T_c and the irreversibility temperature at the given field, T_{irr} , the CESR remains homogeneous and narrows with the lengthening of T_1 . However, below T_{irr} it broadens abruptly and the linewidth depends on the direction of the magnetic field sweep: for up sweeps it is broader than for down sweeps due to the irreversibility of vortex insertion and removal.

To enable a direct measurement of the T_1 spin-lattice relaxation time, one has to resort to time-resolved experiments. Conventional spin-echo ESR methods are limited to T_1 's larger than a few 100 ns. To measure T_1 's of a few nanoseconds, the so-called longitudinally detected ESR was invented in the 1960s by Hervé and Pescia²¹ and improved by several groups.^{22,23} The method is based on the deep amplitude modulation of the microwave excitation with an angular frequency $\Omega \sim 1/T_1$. When the sample is irradiated with the amplitude-modulated microwaves at ESR resonance, the component of the magnetization along the static magnetic field M_z decays from the equilibrium value M_0 with a time constant T_1 . M_z relaxes back to M_0 with a T_1 relaxation time when the microwaves are turned off. The oscillating M_z is detected using a coil which is part of a resonant rf circuit. The phase-sensitive detection of the oscillating voltage using lock-in detection allows the measurement of T_1 using $\Omega T_1 = v/u$,^{5,21} where u and v are the amplitudes of the in- and

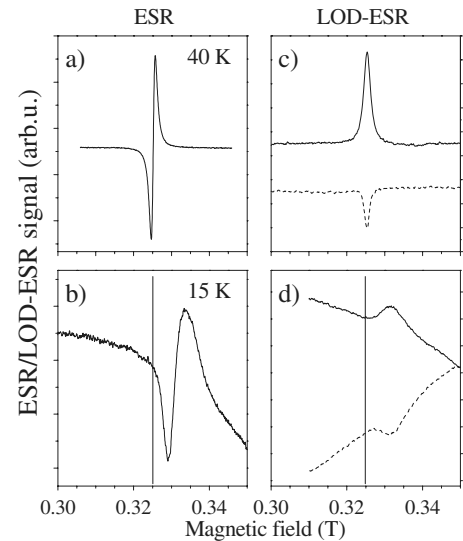


FIG. 4. ESR (a), (b) and LOD ESR (c), (d) spectra of MgB_2 at 9.1 GHz (0.32 T). (a) and (c) at 40 K in the normal state, and (b) and (d) in the superconducting state at 15 K. Solid and dashed curves are the in- and out-of-phase LOD signals, respectively, and are offset for clarity. Vertical solid lines indicate the resonance field above T_c . Note the diamagnetic shift and broadening for both kinds of spectra below T_c . Also note the rotated phase of the in-phase and out-of-phase channels upon cooling.

out-of-phase components of the oscillating magnetization after corrections for instrument related phase shifts. The principal limitation of the LOD ESR technique is its 3–4 orders of magnitude lower sensitivity compared to conventional cw ESR. The LOD ESR method and the experimental apparatus are detailed in Refs. 5 and 6.

To prove that the LOD ESR signal of the itinerant electrons is detected in the superconducting phase, we compare in Fig. 4 the LOD ESR signal with that measured with conventional continuous-wave CESR (referred to as CESR in the following) of MgB_2 in the normal and superconducting states. The CESR signal is the derivative of the absorption due to magnetic field modulation used for lock-in detection. This signal was previously identified as the ESR of conduction electrons in MgB_2 in the superconducting and normal states^{15,17,24} and its characteristics have been discussed in detail.^{15,17} Above T_c at 40 K, the CESR line is relaxationally broadened. Below T_c , it is inhomogeneously broadened and is diamagnetically shifted, i.e., to higher resonance fields. The irreversible effects also contribute to a nonlinear baseline known as the nonresonant microwave absorption.²⁵ The intensity of the CESR signal decreases below T_c as we discussed previously,¹⁷ due to the vanishing of normal state electrons.

The LOD ESR signal shows the same characteristics as the CESR below T_c : it is broadened, shifted to higher fields, and its intensity decreases. The values for the temperature-dependent diamagnetic shifts and broadening and the relative intensity change agree for the two kinds of measurements within experimental precision (not shown). This unambiguously proves that the LOD ESR signal originates from the conduction electrons.

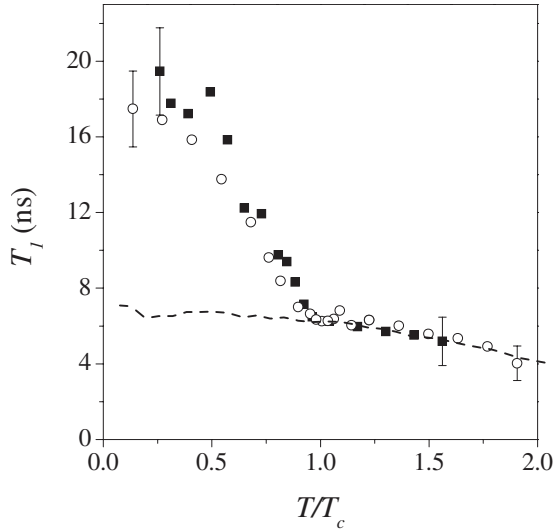


FIG. 5. Spin-lattice relaxation time as a function of the reduced temperature in MgB_2 at 0.32 (■) and 1.27 T (○) magnetic fields. Representative error bars are shown for some of the data. Dashed curve shows T_1 corresponding to ΔH_{hom} in the 15 T measurement as in Fig. 1, with the reduced temperature normalized to 39 K.

The change of the relaxation time T_1 is visible in the LOD ESR spectra in Fig. 4 as a change in the relative intensities of the in- and out-of-phase signals. At 40 K $v/u=0.47$ and at 15 K $v/u=0.95$, which together with $\Omega/2\pi=11.4$ MHz gives 6.3 and 13.3 ns relaxation times, respectively. In Fig. 5, we show the T_1 data inferred from the LOD ESR spectra at 0.32 and 1.27 T as a function of the reduced temperature T/T_c . For MgB_2 , measurement of T_1 is not possible above 60 K due to very short T_1 's and for magnetic fields below ~ 0.3 T due to the large inhomogeneous broadening and the loss of spin susceptibility at the lower magnetic fields below T_c .¹⁷

IV. DISCUSSION

The observed lengthening of T_1 below T_c (Fig. 5) is expected from theory for nonmagnetic scattering centers and low magnetic fields where the susceptibility is dominated by excitations over the superconducting gap. On the other hand, the field independence between 0.32 and 1.27 T of T_1 below T_c is surprising. The lengthening of T_1 below T_c in zero magnetic field for an isotropic, type I superconductor was calculated in the framework of weak-coupled BCS theory by Yafet.³ He concluded that T_1 lengthens as a result of the freezing of normal state excitations. However, no theory exists for a type II superconductor in finite fields with H_{c2} anisotropy such as MgB_2 ; thus here the T_1 data are analyzed phenomenologically in the framework of the two-band or two-gap model of MgB_2 .

In the following, we deduce the residual (low-temperature), impurity-related spin scattering contributions of the σ and π Fermi surface sheets. The DOS is distributed almost equally on the FS sheets of MgB_2 : $N_\pi/(N_\pi+N_\sigma)=0.56$,¹³ where N_π and N_σ are the DOS's of the two types of FS sheets. A magnetic field of ~ 0.3 – 0.4 T closes the gap on

the π FS sheets but leaves the gap on the σ sheet almost intact.^{10,17} This suggests that, well below T_c , our experiment at 0.32 T measures exclusively the relaxation of electrons on the fully closed π FS sheets. Since T_1 at 0.32 T increases slowly with temperature between 10 and 20 K, we extrapolate $T_{1\pi} \approx T_1(10 \text{ K}, 0.32 \text{ T}) = 20(2)$ ns for the π FS.

In order to separate the contribution of the σ FS to the relaxation rate in the normal state, $1/T_{1n}$, we assume that interband relaxation is negligible and $1/T_{1n}$ is equal to the average of the spin-lattice relaxation rates on the two FSs weighted by the corresponding DOS:

$$\frac{1}{T_{1n}} = \frac{N_\pi/T_{1\pi} + N_\sigma/T_{1\sigma}}{N_\pi + N_\sigma}. \quad (1)$$

Here $T_{1\sigma}$ is the spin-lattice relaxation time on the σ FS. The 15 T measurement shows that $1/T_{1n}$ changes little with temperature between 3 and 40 K. Thus we find $T_{1\sigma} = 3.4(5)$ ns for the contribution of the σ FS sheets, using $T_{1n} = T_1(T_c) = 6.3$ ns, $T_{1\pi} = 20(2)$ ns, and Eq. (1).

For normal metals with a simple Fermi surface, the so-called Elliott relation^{2,3,26,27} holds, which states that for a given type of disorder (e.g., phonons or dislocations) T_1 is proportional to the momentum relaxation time τ . The proportionality constant depends on the spin-orbit splitting of the conduction electron bands and has been estimated in a number of metals from the shift of the CESR from the free electron value. Metals with complicated Fermi surfaces, i.e., with great variations of the electron-phonon coupling on the different FS parts are known to deviate from the Elliott relation,²⁸ and calculation of T_1 requires to take into account the details of the band structure.^{29–31} Examples include polyvalent elemental metals such as Mg or Al. Clearly, a calculation of T_1 is required for MgB_2 , which takes into account its band structure peculiarities. Comparison of spin scattering and momentum scattering times of the two types of Fermi surfaces is instructive. The relative values of τ for the two FS parts, τ_π and τ_σ , and for interband scattering were estimated by Mazin *et al.*³² A very small impurity interband scattering and $\tau_\pi < \tau_\sigma$, i.e., a larger π intraband scattering relative to σ intraband scattering was required to explain the rather small depression of T_c in materials with widely different conductivities. de Haas–van Alphen³³ and magnetoresistance³⁴ measurements of high-purity samples yield $\tau_\pi < \tau_\sigma$ also. Such a behavior could arise from Mg vacancies, which perturb more electrons of the π band relative to the σ band. However, our spin scattering data do not support this. In contrast to momentum scattering, spin scattering is stronger on the σ FS: $T_{1\pi}:T_{1\sigma}=6:1$ in high-purity samples and at low temperatures. The relative values of T_1 and τ for the two FS's do not necessarily follow the same trend; spin relaxation times at low temperatures depend on the spin-orbit interaction on impurities while momentum relaxation is due to potential scattering. However, a defect center such as a Mg vacancy with a strong modification of the electron-phonon coupling would greatly affect T_1 compared to τ . In the two-band model, Mg defects are expected to shorten $T_{1\pi}$ more than $T_{1\sigma}$ and thus are unlikely to be the dominant scatterers.

A final note concerns the validity of the above analysis of T_1 's in the framework of the two-band or gap model. The field independence of the lowest temperature T_1 for 0.32 and 1.27 T is unexpected within this model. The spin susceptibility increases strongly between these fields, and more normal states are restored at 1.27 T than expected from the closing of the gap on the π FS sheets alone.¹⁷ Based on this, one would expect to observe additional spin scattering from the restored σ FS parts, which is clearly not the case. This also indicates that a theoretical study which takes into account the peculiarities of MgB_2 is required to explain the anomalous spin-lattice relaxation times.

In conclusion, we presented the measurement of the spin-lattice relaxation time T_1 of conduction electrons as a function of temperature and magnetic field in the MgB_2 superconductor. We use a method based on the detection of the z component of the conduction electron magnetization during electron-spin-resonance conditions with amplitude-modulated microwave excitation. Lengthening of T_1 below

T_c is observed irrespective of the significant CESR line broadening due to irreversible diamagnetism in the polycrystalline sample. The field independence of T_1 for 0.32 and 1.27 T allows us to measure the separate contributions to T_1 from the two distinct types of the Fermi surface.

ACKNOWLEDGMENTS

The authors are grateful to Richárd Gaál for the development of the ESR instrument at the EPFL. F.S. acknowledges the Zoltán Magyary foundation and the Bolyai program of the Hungarian Academy of Sciences. F.M. acknowledges the Alexander von Humboldt Foundation for support. The work was supported by the Hungarian State (OTKA) Grant Nos. TS049881, F61733, PF63954, and NK60984 and by the Swiss NSF and its NCCR "MaNEP." Ames Laboratory is operated for the U.S. Department of Energy by Iowa State University under Contract No. W-7405-Eng-82.

*Corresponding author. simon@esr.phy.bme.hu

[†]Present address: Leibniz Institute for Solid State and Materials Research Dresden, PF 270116 D-01171 Dresden, Germany.

[‡]Present address: Condensed Matter Physics and Materials Science Department, Brookhaven National Laboratory, Upton, New York 11973-5000, USA.

¹I. Žutić, J. Fabian, and S. D. Sarma, *Rev. Mod. Phys.* **76**, 323 (2004).

²R. J. Elliott, *Phys. Rev.* **96**, 266 (1954).

³Y. Yafet, *Phys. Lett.* **98A**, 287 (1983).

⁴N. M. Nemes, J. E. Fischer, G. Baumgartner, L. Forró, T. Fehér, G. Oszlányi, F. Simon, and A. Jánossy, *Phys. Rev. B* **61**, 7118 (2000).

⁵F. Murányi, F. Simon, F. Fülöp, and A. Jánossy, *J. Magn. Reson.* **167**, 221 (2004).

⁶F. Simon and F. Murányi, *J. Magn. Reson.* **173**, 288 (2005).

⁷J. Nagamatsu, N. Nakagawa, T. Muranaka, Y. Zenitani, and J. Akimitsu, *Nature (London)* **410**, 63 (2001).

⁸F. Bouquet, R. A. Fisher, N. E. Phillips, D. G. Hinks, and J. D. Jorgensen, *Phys. Rev. Lett.* **87**, 047001 (2001).

⁹P. Szabó, P. Samuely, J. Kacmarčík, T. Klein, J. Marcus, D. Fruchart, S. Miraglia, C. Marcenat, and A. G. M. Jansen, *Phys. Rev. Lett.* **87**, 137005 (2001).

¹⁰F. Bouquet, Y. Wang, I. Sheikin, T. Plackowski, A. Junod, S. Lee, and S. Tajima, *Phys. Rev. Lett.* **89**, 257001 (2002).

¹¹S. Tsuda, T. Yokoya, Y. Takano, H. Kito, A. Matsushita, F. Yin, J. Itoh, H. Harima, and S. Shin, *Phys. Rev. Lett.* **91**, 127001 (2003).

¹²J. Kortus, I. I. Mazin, K. D. Belashchenko, V. P. Antropov, and L. L. Boyer, *Phys. Rev. Lett.* **86**, 4656 (2001).

¹³H. J. Choi, D. Roundy, H. Sun, M. L. Cohen, and S. G. Louie, *Nature (London)* **418**, 758 (2002).

¹⁴M. R. Eskildsen, M. Kugler, S. Tanaka, J. Jun, S. M. Kazakov, J. Karpinski, and Ø. Fischer, *Phys. Rev. Lett.* **89**, 187003 (2002).

¹⁵F. Simon *et al.*, *Phys. Rev. Lett.* **87**, 047002 (2001).

¹⁶M. Angst, R. Puzniak, A. Wisniewski, J. Jun, S. M. Kazakov, J. Karpinski, J. Roos, and H. Keller, *Phys. Rev. Lett.* **88**, 167004 (2002).

¹⁷F. Simon, A. Jánossy, T. Fehér, F. Murányi, S. Garaj, L. Forró, C. Petrovic, S. L. Bud'ko, R. A. Ribeiro, and P. C. Canfield, *Phys. Rev. B* **72**, 012511 (2005).

¹⁸F. J. Dyson, *Phys. Rev.* **98**, 349 (1955).

¹⁹D. K. Finnemore, J. E. Ostenson, S. L. Bud'ko, G. Lapertot, and P. C. Canfield, *Phys. Rev. Lett.* **86**, 2420 (2001).

²⁰P. Pincus, *Phys. Lett.* **13**, 21 (1964).

²¹J. Hervé and J. Pescia, *C. R. Hebd. Seances Acad. Sci.* **251**, 665 (1960).

²²V. A. Atsarkin, V. V. Demidov, and G. A. Vasneva, *Phys. Rev. B* **52**, 1290 (1995).

²³J. Granwehr, J. Forrer, and A. Schweiger, *J. Magn. Reson.* **151**, 78 (2001).

²⁴R. R. Urbano, P. G. Pagliuso, C. Rettori, Y. Kopelevich, N. O. Moreno, and J. L. Sarrao, *Phys. Rev. Lett.* **89**, 087602 (2002).

²⁵K. W. Blazey, K. A. Müller, J. G. Bednorz, W. Berlinger, G. Amoretti, E. Buluggiu, A. Vera, and F. C. Matocotta, *Phys. Rev. B* **36**, 7241 (1987).

²⁶Y. Yafet, in *Solid State Physics*, edited by F. Seitz and D. Turnbull (Academic Press, New York, 1963), Vol. 14, p. 1.

²⁷F. Beuneu and P. Monod, *Phys. Rev. B* **18**, 2422 (1977).

²⁸P. Monod and F. Beuneu, *Phys. Rev. B* **19**, 911 (1979).

²⁹R. H. Silsbee and F. Beuneu, *Phys. Rev. B* **27**, 2682 (1983).

³⁰J. Fabian and S. Das Sarma, *Phys. Rev. Lett.* **81**, 5624 (1998).

³¹J. Fabian and S. Das Sarma, *Phys. Rev. Lett.* **83**, 1211 (1999).

³²I. I. Mazin, O. K. Andersen, O. Jepsen, O. V. Dolgov, J. Kortus, A. A. Golubov, A. B. Kuz'menko, and D. van der Marel, *Phys. Rev. Lett.* **89**, 107002 (2002).

³³E. A. Yelland, J. R. Cooper, A. Carrington, N. E. Hussey, P. J. Meeson, S. Lee, A. Yamamoto, and S. Tajima, *Phys. Rev. Lett.* **88**, 217002 (2002).

³⁴I. Pallecchi *et al.*, *Phys. Rev. B* **72**, 184512 (2005).